Adaptive 2D IGA boundary element methods

Michael Feischl, Gregor Gantner*, Alexander Haberl, Dirk Praetorius

Abstract

We derive and discuss a posteriori error estimators for Galerkin and collocation IGA boundary element methods for weakly-singular integral equations of the first-kind in 2D. While recent own work considered the Faermann residual error estimator for Galerkin IGA boundary element methods, the present work focuses more on collocation and weighted-residual error estimators, which provide reliable upper bounds for the energy error. Our analysis allows piecewise smooth parametrizations of the boundary, local mesh-refinement, and related standard piecewise polynomials as well as NURBS. We formulate an adaptive algorithm which steers the local mesh-refinement and the multiplicity of the knots. Numerical experiments show that the proposed adaptive strategy leads to optimal convergence, and related IGA boundary element methods are superior to standard boundary element methods with piecewise polynomials.

Keywords: isogeometric analysis, boundary element method, collocation, a posteriori error estimate, adaptive mesh-refinement

1. Introduction

1.1. Isogeometric analysis

The central idea of isogeometric analysis (IGA) is to use the same ansatz functions for the discretization of the partial differential equation at hand as for the representation of the problem geometry. Usually, Ω is represented in computer aided design (CAD) by means of NURBS, hierarchical splines, or T-splines. This concept, invented in [HCB05] for finite element methods (IGAFEM) has proved very fruitful in applications [HCB05, SBTR12]; see also the monograph [CHB09]. Since CAD directly provides a parametrization of the boundary $\partial\Omega$, this makes the boundary element method (BEM) the most attractive numerical scheme, if applicable (i.e., provided that the fundamental solution of the differential operator is explicitly known). Isogeometric BEM (IGABEM) has first been considered in [PGK+09] for 2D resp. [SSE+13] for 3D. While standard BEM with piecewise polynomials is well-studied in the literature, cf. the monographs [SS11, Ste08] and the references therein, the numerical analysis of IGA-BEM is essentially open. We refer to [SBTR12, TM12, PTC13] for numerical experiments and to [HAD14] for some quadrature analysis. A posteriori error estimation has first been considered for Galerkin IGABEM in our recent work [FGP15]. In the present work, we extend the latter result to collocation IGABEM which is preferred in practice for its simpler assembly of the stiffness matrix.

1.2. Model problem

Let $\Omega \subset \mathbb{R}^2$ be a Lipschitz domain and $\Gamma \subseteq \partial\Omega$ be a compact, piecewise smooth part of the boundary with finitely many connected components. For a given right-hand side f, we consider the weakly-singular boundary integral equation

$$V\phi(x) := -\frac{1}{2\pi}\int_\Gamma \log|x-y|\,\phi(y)\,dy = f(x) \quad \text{on } \Gamma \quad (1.1)$$

associated with the 2D Laplacian; see Section 2 below for the mathematical setting and the definition of the problem related energy norm $\|\!|\cdot|\!\|$. With some discrete ansatz space $\mathcal{X}_h \subset L^2(\Gamma)$, the Galerkin BEM computes the unique solution $\phi_h \in \mathcal{X}_h$ of the discrete variational formulation

$$\int_\Gamma V\phi_h\,\psi_h\,dx = \int_\Gamma f\psi_h\,dx \quad \text{for all } \psi_h \in \mathcal{X}_h. \quad (1.2)$$

Note that $\mathcal{X}_h \subset L^2(\Gamma)$ ensures $V\phi_h \in C(\Gamma)$. The collocation BEM computes $\phi_h \in \mathcal{X}_h$ such that

$$V\phi_h(x_j) = f(x_j) \quad \text{for all } x_j \in \{x_1, \ldots, x_{N_{\text{col}}}\}, \quad (1.3)$$

where the x_j are appropriately chosen collocation points with $N_{\text{col}} := \dim \mathcal{X}_h$; see Section 2.8. In either case (1.2)–(1.3), ϕ_h is computed by solving a linear system of equations

1.3. A posteriori error estimation for Galerkin IGABEM

We assume that $\mathcal{X}_h$ is associated to some partition $\mathcal{T}_h$ of Γ into a set of connected segments. For each vertex z of $\mathcal{T}_h$, let $\omega_h(z) := \bigcup\{T \in \mathcal{T}_h : z \in T\}$ denote the node patch. If $\mathcal{X}_h$ is sufficiently rich (e.g., $\mathcal{X}_h$ contains certain

---

*Corresponding Author

Email addresses: `Michael.Feischl@tuwien.ac.at` (Michael Feischl), `Gregor.Gantner@tuwien.ac.at` (Gregor Gantner), `Alexander.e101.Haberl@tuwien.ac.at` (Alexander Haberl), `Dirk.Praetorius@tuwien.ac.at` (Dirk Praetorius)

splines or NURBS), it is proved in [FGP15] that Galerkin BEM guarantees reliability and efficiency

$$C_{\mathrm{rel}}^{-1} \|\phi - \phi_h\| \le \eta_h := \Big(\sum_{z \in \mathcal{N}_h} \eta_h(z)^2 \Big)^{1/2} \tag{1.4a}$$

$$\le C_{\mathrm{eff}} \|\phi - \phi_h\|$$

with $\mathcal{X}_h$-independent constants $C_{\mathrm{eff}}, C_{\mathrm{rel}} > 0$. Here, $r_h := f - V\phi_h$ denotes the residual and

$$\eta_h(z)^2 := \int_{\omega_h(z)} \int_{\omega_h(z)} \frac{|r_h(x) - r_h(y)|^2}{|x - y|^2} \, dy \, dx \tag{1.4b}$$

is some Sobolev-Slobodeckij seminorm, i.e., the unknown BEM energy error is controlled by some computable a posteriori error estimator η_h. Estimate (1.4) has first been proved by Faermann [Fae00] for closed $\Gamma = \partial\Omega$ and standard spline spaces $\mathcal{X}_h$ based on the arclength parametrization. Her result is generalized in [FGP15] to a more general setting which also includes isogeometric analysis. We note that [Fae00, FGP15] show that the efficiency estimate $\eta_h \le C_{\mathrm{eff}} \|\phi - \phi_h\|$ holds even independently of the discretization and, in particular, for collocation.

1.4. A posteriori error estimation for collocation IGABEM

In the present manuscript, we focus on the weighted-residual error estimator which has first been proposed in [CS96, Car97] for standard BEM with piecewise polynomials and polygonal Γ. We prove that for Galerkin IGABEM (1.2) as well as collocation IGABEM (1.3), there holds the upper bound

$$C_{\mathrm{rel}}^{-1} \|\phi - \phi_h\| \le \mu_h := \Big(\sum_{z \in \mathcal{N}_h} \mu_h(z)^2 \Big)^{1/2}, \tag{1.5a}$$

with an $\mathcal{X}_h$-independent constant $C_{\mathrm{rel}} > 0$. Here, $r_h := f - V\phi_h$ is again the residual and

$$\mu_h(z)^2 := |\omega_h(z)| \int_{\omega_h(z)} |r_h'(x)|^2 \, dx \tag{1.5b}$$

is a weighted H^1-seminorm, where $(\cdot)'$ denotes the arclength derivative and $|\omega_h(z)|$ is the length of the node patch. For collocation BEM, we thus control the energy error by

$$C_{\mathrm{eff}}^{-1} \eta_h \le \|\phi - \phi_h\| \le C_{\mathrm{rel}} \mu_h \tag{1.6}$$

which, however, involves different error estimators. In addition to the global relation of the error estimators η_h and μ_h and independently of the discretization, we prove

$$\eta_h(z) \le C_{\mathrm{loc}} \mu_h(z) \quad \text{for all vertices } z \text{ of } \mathcal{T}_h, \tag{1.7}$$

where $C_{\mathrm{loc}} > 0$ depends only on Γ.

1.5. Outline

Section 2 recalls the functional analytic framework, provides the assumptions on Γ and its parametrization γ, introduces the ansatz spaces, and presents an adaptive algorithm which is capable to control and adapt the multiplicity of the nodes as well as the local mesh-size (Algorithm 2.2). Section 3 provides the numerical evidence that the proposed adaptive IGABEM is superior to IGABEM with uniform mesh-refinement as well as to adaptive standard BEM with piecewise polynomials. Moreover, we observe that collocation IGABEM leads to essentially the same convergence behavior as Galerkin IGABEM, so that an adaptive collocation IGABEM may be favorable in practice. Section 4 recalls the precise statement of (1.4) from [FGP15] and gives a proof of (1.5)–(1.7). The concluding Section 5 comments on our overall findings, open questions, and future research.

2. Preliminaries

In this section, we collect the main assumptions on the boundary and its discretization and introduce the BEM ansatz spaces. Further details on Sobolev spaces and the functional analytic setting of weakly-singular integral equations, are found, e.g., in the monographs [HW08, McL00, SS11] and the references therein.

Throughout, $|\cdot|$ denotes the absolute value of scalars, the Euclidean norm of vectors in $\mathbb{R}^2$, the measure of a set in $\mathbb{R}$ (e.g., the length of an interval), or the arclength of a curve in $\mathbb{R}^2$. The respective meaning will be clear from the context.

We write $A \lesssim B$ to abbreviate $A \le cB$ with some constant $c > 0$ which is clear from the context. Moreover $A \simeq B$ abbreviates $A \lesssim B \lesssim A$.

2.1. Function spaces

For any measurable subset $\omega \subseteq \Gamma$ resp. any interval $\omega \subseteq \mathbb{R}$, $L^2(\omega)$ denotes the Lebesgue space of all square integrable functions with corresponding norm

$$\|u\|_{L^2(\omega)}^2 := \int_\omega |u(x)|^2 \, dx. \tag{2.1}$$

If $u \in L^2(\omega)$ is differentiable along the arc, u' denotes the arclength derivative. Define the Sobolev space $H^1(\omega) := \{u \in L^2(\omega) : u' \in L^2(\omega)\}$ with corresponding norm

$$\|u\|_{H^1(\omega)}^2 := \|u\|_{L^2(\omega)}^2 + |u|_{H^1(\omega)}^2, \tag{2.2a}$$

$$|u|_{H^1(\omega)}^2 := \int_\omega |u'(x)|^2 \, dx. \tag{2.2b}$$

Furthermore, define the Sobolev space $H^{1/2}(\omega) := \{u \in L^2(\omega) : \|u\|_{H^{1/2}(\omega)} < \infty\}$ with corresponding norm

$$\|u\|_{H^{1/2}(\omega)}^2 := \|u\|_{L^2(\omega)}^2 + |u|_{H^{1/2}(\omega)}^2, \tag{2.3a}$$

$$|u|_{H^{1/2}(\omega)}^2 := \int_\omega \int_\omega \frac{|u(x) - u(y)|^2}{|x - y|^2} \, dy \, dx. \tag{2.3b}$$

The dual space of $H^{1/2}(\omega)$ is $\widetilde{H}^{-1/2}(\omega)$, where duality is understood with respect to the extended $L^2(\omega)$-scalar product, i.e., for $u \in H^{1/2}(\omega)$ and $\phi \in L^2(\omega)$, it holds

$$\langle u \,;\, \phi \rangle_\omega = \int_\omega u(x)\phi(x)\, dx. \qquad (2.4)$$

We note that $H^{1/2}(\Gamma) \subset L^2(\Gamma) \subset \widetilde{H}^{-1/2}(\Gamma)$ form a Gelfand triple and all inclusions are dense and compact.

Amongst other equivalent definitions of $H^{1/2}(\omega)$ are the characterization as trace space of functions in $H^1(\Omega)$ as well as equivalent interpolation techniques. All these definitions provide the same space but different norms, where norm equivalence constants depend only on ω.

2.2. Weakly-singular integral equation

The operator V from (1.1) extends to a linear and continuous operator $V : \widetilde{H}^{-1/2}(\Gamma) \to H^{1/2}(\Gamma)$ with additional stability $V : L^2(\Gamma) \to H^1(\Gamma)$. We additionally suppose that V is even an elliptic isomorphism, which is satisfied, e.g., if $\mathrm{diam}(\Omega) < 1$. In particular, $\langle V(\cdot) \,;\, (\cdot) \rangle_\Gamma$ is thus a scalar product on $\widetilde{H}^{-1/2}(\Gamma)$, and the induced energy norm

$$\|\psi\|^2 := \langle V\psi \,;\, \psi \rangle_\Gamma \quad \text{for } \psi \in \widetilde{H}^{-1/2}(\Gamma) \qquad (2.5)$$

is an equivalent norm on $\widetilde{H}^{-1/2}(\Gamma)$.

Given $f \in H^{1/2}(\Gamma)$, the weakly-singular integral equation (1.1) is equivalently reformulated in variational form: Find $\phi \in \widetilde{H}^{-1/2}(\Gamma)$ such that

$$\langle V\phi \,;\, \psi \rangle_\Gamma = \langle f \,;\, \psi \rangle_\Gamma \quad \text{for all } \psi \in \widetilde{H}^{-1/2}(\Gamma). \qquad (2.6)$$

The Lax-Milgram lemma thus applies and proves existence and uniqueness of the solution $\phi \in \widetilde{H}^{-1/2}(\Gamma)$ of (2.6) resp. (1.1).

2.3. Parametrization of boundary

Let $\Gamma = \bigcup_i \Gamma_i \subseteq \partial\Omega$ be decomposed into its finitely many connected components Γ_i. Then,

$$\|u\|^2_{H^{1/2}(\Gamma)} \simeq \sum_i \|u\|^2_{H^{1/2}(\Gamma_i)} \quad \text{for all } u \in H^{1/2}(\Gamma);$$

see, e.g., [FGP15, Section 2.2]. The usual piecewise polynomial and NURBS basis functions have connected support and are hence supported by some *single* Γ_i each. Without loss of generality and to ease the mathematical proofs, we may therefore assume that Γ is connected. All results remain valid for non-connected Γ.

We assume that either $\Gamma = \partial\Omega$ is parametrized by a closed continuous and piecewise two times continuously differentiable path $\gamma : [a,b] \to \Gamma$ such that the restriction $\gamma|_{[a,b)}$ is even bijective, or that $\Gamma \subsetneqq \partial\Omega$ is parametrized by a bijective continuous and piecewise two times continuously differentiable path $\gamma : [a,b] \to \Gamma$. For $\Gamma = \partial\Omega$, we denote the $(b-a)$-periodic extension to $\mathbb{R}$ also by γ. For the left and right derivative of γ, we assume that $\gamma'^\ell(t) \neq 0$ for

$t \in (a,b]$ and $\gamma'^r(t) \neq 0$ for $t \in [a,b)$. Moreover we assume that $\gamma'^\ell(t) + c\gamma'^r(t) \neq 0$ for all $c > 0$ and $t \in [a,b]$ resp. $t \in (a,b)$.

By $\gamma_L : [0,L] \to \Gamma$, we denote the arclength parametrization, i.e., $|\gamma_L'^\ell(t)| = 1 = |\gamma_L'^r(t)|$, and its periodic extension. Then, elementary differential geometry yields bi-Lipschitz continuity

$$C_\Gamma^{-1} \le \frac{|\gamma_L(s) - \gamma_L(t)|}{|s-t|} \le C_\Gamma \quad \text{for all } s,t \in \mathbb{R},$$
$$\text{with } \begin{cases} |s-t| \le \frac{3}{4}L, & \text{for } \Gamma = \partial\Omega, \\ s \neq t \in [0,L], & \text{for } \Gamma \subsetneqq \partial\Omega; \end{cases} \qquad (2.7)$$

see, e.g., [Gan14, Lemma 2.1] for the proof for $\Gamma = \partial\Omega$ which even simplifies for $\Gamma \subsetneqq \partial\Omega$. Let $I \subseteq [a,b]$. Suppose $|I| \le \frac{3}{4}L$ for $\Gamma = \partial\Omega$. Then, (2.7) implies

$$C_\Gamma^{-1} |u \circ \gamma_L|_{H^{1/2}(I)} \le |u|_{H^{1/2}(\gamma_L(I))}$$
$$\le C_\Gamma |u \circ \gamma_L|_{H^{1/2}(I)} \qquad (2.8)$$

for all $u \in H^{1/2}(\Gamma)$.

2.4. Discretization of boundary

For the discretization, let $\mathcal{T}_h = \{T_1, \ldots, T_n\}$ be a partition of Γ into compact and connected segments T_j. The endpoints of the elements of $\mathcal{T}_h$ form the set of nodes

$$\mathcal{N}_h = \begin{cases} \{z_j \,:\, j = 1, \ldots, n\} & \text{for } \Gamma = \partial\Omega, \\ \{z_j \,:\, j = 0, \ldots, n\} & \text{for } \Gamma \subsetneqq \partial\Omega. \end{cases}$$

The arclength of each element $T \in \mathcal{T}_h$ is denoted by h_T. Moreover, the shape regularity constant is defined by

$$\kappa(\mathcal{T}_h) := \max\{h_T/h_{T'} \,:\, T, T' \in \mathcal{T}_h, T \cap T' \neq \emptyset\}.$$

For $\Gamma = \partial\Omega$, we extend the nodes, elements, and their length periodically. Moreover, we suppose

$$\max_{T \in \mathcal{T}_h} h_T \le |\Gamma|/4 \quad \text{for } \Gamma = \partial\Omega. \qquad (2.9)$$

2.5. Discretization of parameter domain

Given $\gamma : [a,b] \to \Gamma$, the partition $\mathcal{T}_h$ induces a partition $\check{\mathcal{T}}_h = \{\check{T}_1, \ldots, \check{T}_n\}$ of the parameter domain $[a,b]$. Let $a = \check{z}_0 < \check{z}_1 < \cdots < \check{z}_n = b$ be the endpoints of the elements of $\check{\mathcal{T}}_h$. We assume $\check{T}_j = [\check{z}_{j-1}, \check{z}_j]$, $\gamma(\check{T}_j) = T_j$, and $\gamma(\check{z}_j) = z_j$. We define

$$\check{\mathcal{N}}_h = \begin{cases} \{\check{z}_j \,:\, j = 1, \ldots, n\} & \text{for } \Gamma = \partial\Omega, \\ \{\check{z}_j \,:\, j = 0, \ldots, n\} & \text{for } \Gamma \subsetneqq \partial\Omega. \end{cases}$$

The length of each $\check{T} \in \check{\mathcal{T}}_h$ is denoted by $h_{\check{T}}$. Moreover, we define the shape regularity constant on $[a,b]$ by

$$\kappa(\check{\mathcal{T}}_h) := \max\{h_{\check{T}}/h_{\check{T}'} \,:\, \check{T}, \check{T}' \in \check{\mathcal{T}}_h, \gamma(\check{T}) \cap \gamma(\check{T}') \neq \emptyset\}.$$

Note that $\kappa(\mathcal{T}_h) \simeq \kappa(\check{\mathcal{T}}_h)$, where the hidden constants depend only on the parametrization γ.

2.6. B-splines and NURBS in the parameter domain

We consider *knots* $\check{\mathcal{K}} := (t_i)_{i \in \mathbb{Z}}$ on $\mathbb{R}$ with $t_{i-1} \leq t_i$ for $i \in \mathbb{Z}$ and $\lim_{i \to \pm\infty} t_i = \pm\infty$. For the multiplicity of any knot t_i, we write $\#t_i$. We denote the corresponding set of *nodes* $\check{\mathcal{N}} := \{t_i : i \in \mathbb{Z}\} = \{\check{z}_j : j \in \mathbb{Z}\}$ with $\check{z}_{j-1} < \check{z}_j$ for all $j \in \mathbb{Z}$. For $i \in \mathbb{Z}$ and $p \in \mathbb{N}_0$, the i-th *B-Spline* of degree p is defined inductively by

$$B_{i,p}^{\check{\mathcal{K}}} := B_{i,p} := \begin{cases} \chi_{[t_{i-1}, t_i)} & \text{for } p = 0, \\ \beta_{i-1,p} B_{i,p-1} + (1 - \beta_{i,p}) B_{i+1,p-1} & \text{for } p > 0, \end{cases}$$

where, for $t \in \mathbb{R}$,

$$\beta_{i,p}(t) := \begin{cases} \frac{t - t_i}{t_{i+p} - t_i} & \text{for } t_i \neq t_{i+p}, \\ 0 & \text{for } t_i = t_{i+p}. \end{cases}$$

We collect some basic properties of B-splines from [dB86]:

Lemma 2.1 ([dB86, Theorem 6, Section 2 and page 9–10]). *For $p \in \mathbb{N}_0$, the following assertions hold:*

(i) *Let $I = [a, b]$ be a finite interval. Then,*

$$\{B_{i,p}|_I : i \in \mathbb{Z}, B_{i,p}|_I \neq 0\} \tag{2.10}$$

is a basis for the space of all right-continuous $\check{\mathcal{N}}$-piecewise polynomials of degree lower or equal p on I and which are, at each knot t_i, $p - \#t_i$ times continuously differentiable if $p - \#t_i \geq 0$.

(ii) *For $i \in \mathbb{Z}$, $B_{i,p}$ vanishes outside the interval $[t_{i-1}, t_{i+p}]$. It is positive on the open interval (t_{i-1}, t_{i+p}).*

(iii) *For $i \in \mathbb{Z}$, $B_{i,p}$ is completely determined by the $p + 2$ knots $t_{i-1}, \ldots, t_{i+p}$.*

(iv) *The B-splines of degree p form a locally finite partition of unity, i.e., $\sum_{i \in \mathbb{Z}} B_{i,p} = 1$ on $\mathbb{R}$.* $\square$

In addition to the knots $\check{\mathcal{K}} = (t_i)_{i \in \mathbb{Z}}$, we consider weights $\mathcal{W} := (w_i)_{i \in \mathbb{Z}}$ with $w_i > 0$. For $i \in \mathbb{Z}$ and $p \in \mathbb{N}_0$, we define the i-th *non-uniform rational B-Spline* (*NURBS*) of degree p

$$R_{i,p}^{\check{\mathcal{K}}, \mathcal{W}} := R_{i,p} := \frac{w_i B_{i,p}}{\sum_{\ell \in \mathbb{Z}} w_\ell B_{\ell,p}}. \tag{2.11}$$

Note that the denominator is positive and locally finite.

For any $p \in \mathbb{N}_0$, we define the vector spaces

$$\mathscr{S}^p(\check{\mathcal{K}}) := \left\{ \sum_{i \in \mathbb{Z}} a_i B_{i,p}^{\check{\mathcal{K}}} : a_i \in \mathbb{R} \right\}, \tag{2.12}$$

$$\mathscr{N}^p(\check{\mathcal{K}}, \mathcal{W}) := \left\{ \sum_{i \in \mathbb{Z}} a_i R_{i,p}^{\check{\mathcal{K}}, \mathcal{W}} : a_i \in \mathbb{R} \right\}. \tag{2.13}$$

2.7. NURBS on the boundary

For $\Gamma = \partial\Omega$, each node $\check{z} \in \check{\mathcal{N}}_h$ has a multiplicity $\#\check{z} \leq p + 1$. This induces a sequence of non-decreasing knots $\check{\mathcal{K}}_h = (t_i)_{i=1}^N$ on (a, b). Let $\mathcal{W}_h = (w_i)_{i=1}^N$ be a sequence of weights on these knots. We extend the knot sequence $(b - a)$-periodically to $(t_i)_{i \in \mathbb{Z}}$ and the weight sequence to $(w_i)_{i \in \mathbb{Z}}$ by $w_{N+i} := w_i$ for $i \in \mathbb{Z}$. For the extended sequences, we also write $\check{\mathcal{K}}_h$ and $\mathcal{W}_h$. We set

$$\widehat{\mathscr{N}^p}(\check{\mathcal{K}}_h, \mathcal{W}_h) := \mathscr{N}^p(\check{\mathcal{K}}_h, \mathcal{W}_h)|_{[a,b]} \circ \gamma|_{[a,b]}^{-1}. \tag{2.14}$$

For $\Gamma \subsetneq \partial\Omega$, each node $\check{z} \in \check{\mathcal{N}}_h$ has a multiplicity $\#\check{z} \leq p + 1$ such that $\#\check{z}_0 = \#\check{z}_n = p + 1$. This induces a sequence of non-decreasing knots $\check{\mathcal{K}}_h = (t_i)_{i=-p}^N$ on $[a, b]$. Let $\mathcal{W}_h = (w_i)_{i=1}^N$ be a sequence of weights. We extend the sequences arbitrarily to $\check{\mathcal{K}}_h = (t_i)_{i \in \mathbb{Z}}$ with $t_i \leq t_{i+1}$ for $i \in \mathbb{Z}$, $a > t_i \to -\infty$ for $i < -p$, and $b < t_i \to \infty$ for $i > N$, and $\mathcal{W}_h = (w_i)_{i \in \mathbb{Z}}$ with $w_i > 0$. We set

$$\widehat{\mathscr{N}^p}(\check{\mathcal{K}}_h, \mathcal{W}_h) := \mathscr{N}^p(\check{\mathcal{K}}_h, \mathcal{W}_h)|_{[a,b]} \circ \gamma^{-1}. \tag{2.15}$$

Due to Lemma 2.1 (ii)–(iii), this definition does not depend on how the sequences are extended.

2.8. Collocation IGABEM

In this section, we show how to choose the collocation points x_j for $j = 1, \ldots, N_{\text{col}}$ in (1.3). First, we note that Lemma 2.1 (i) implies that

$$\{R_{i,p}|_{(a,b)} : i = 1 - p, \ldots, N - \#b + 1\} \circ \gamma|_{[a,b)}^{-1} \tag{2.16}$$

for $\Gamma = \partial\Omega$ resp.

$$\{R_{i,p}|_{[a,b]} : i = 1 - p, \ldots, N - p\} \circ \gamma^{-1} \tag{2.17}$$

for $\Gamma \subsetneq \partial\Omega$ forms a basis of $\widehat{\mathscr{N}^p}(\check{\mathcal{K}}_h, \mathcal{W}_h)$. Recall $\#b = p + 1$ for $\Gamma \subsetneq \partial\Omega$. For simplicity, suppose $\#b = p + 1$ also for $\Gamma = \partial\Omega$. This gives

$$N_{\text{col}} = N. \tag{2.18}$$

For $j = 1, \ldots, N$, the collocation point x_j is defined through the arithmetic mean of $p+2$ knots in the parameter domain

$$x_j = \gamma(\check{x}_j) \quad \text{with} \quad \check{x}_j := \frac{\sum_{k=j-p-1}^j t_k}{p + 2}. \tag{2.19}$$

2.9. Adaptive algorithm

Finally, we recall an adaptive algorithm from our preceding work [FGP15], which steers the h-refinement of the partition $\mathcal{T}_h$ as well as the increase of the multiplicity of the nodes $\mathcal{N}_h$. While [FGP15] considered η_h for Galerkin IGABEM, the current focus is on μ_h and collocation IGABEM.

Suppose that Γ is represented by a NURBS curve of degree $p \in \mathbb{N}_0$. This induces the initial partition $\mathcal{T}_0$ of Γ with nodes $\mathcal{N}_0$, related nodes $\check{\mathcal{N}}_0$ in the parameter domain, and positive weights $\mathcal{W}_0$. Each node has a multiplicity

lower or equal $p + 1$, where for $\Gamma \subsetneq \partial\Omega$ or collocation IGABEM we suppose $\#a = \#b = p + 1$. For $\Gamma = \partial\Omega$, we suppose $h_T \leq |\Gamma|/4$ for all $T \in \mathcal{T}_0$.

As the initial trial space, we consider

$$\widehat{\mathscr{N}^p}(\check{\mathcal{K}}_0, \mathcal{W}_0) \subset L^2(\Gamma) \subset H^{-1/2}(\Gamma). \tag{2.20}$$

Fix an error estimator $\varrho_h \in \{\eta_h, \mu_h\}$. The nodal contributions $\varrho_h(z)$ from (1.4) resp. (1.5) are used to steer knot insertion from $\check{\mathcal{K}}_h$ to the following knots $\check{\mathcal{K}}_H$. The new weights $\mathcal{W}_H$ are uniquely chosen such that the denominator of the NURBS functions does not change. In particular, this implies nestedness

$$\widehat{\mathscr{N}^p}(\check{\mathcal{K}}_h, \mathcal{W}_h) \subseteq \widehat{\mathscr{N}^p}(\check{\mathcal{K}}_H, \mathcal{W}_H) \tag{2.21}$$

of the related NURBS spaces. Since the weights in $\mathcal{W}_H$ are just convex combinations of the weights in $\mathcal{W}_0$, it holds $\min \mathcal{W}_0 \leq \min \mathcal{W}_H \leq \max \mathcal{W}_H \leq \max \mathcal{W}_0$. For details, we refer to [FGP15, Section 4.2].

Then, the adaptive algorithm reads as follows:

Algorithm 2.2. *Input: Adaptivity parameter $0 < \theta \leq 1$, polynomial order $p \in \mathbb{N}_0$, initial partition $\mathcal{T}_0 = \mathcal{T}_h$ with knots $\check{\mathcal{K}}_0 = \check{\mathcal{K}}_h$, initial weights $\mathcal{W}_0 = \mathcal{W}_h$.*
Adaptive loop: Iterate the following steps (i)–(vi), *until ϱ_h is sufficiently small:*

(i) *Compute approximation $\phi_h \in \widehat{\mathscr{N}^p}(\check{\mathcal{K}}_h, \mathcal{W}_h)$ from Galerkin BEM (1.2) resp. collocation BEM (1.3).*

(ii) *Compute indicators $\varrho_h(z)$ for all nodes $z \in \mathcal{N}_h$.*

(iii) *Determine a set $\mathcal{M}_h \subseteq \mathcal{N}_h$ of minimal cardinality such that*

$$\theta \varrho_h^2 \leq \sum_{z \in \mathcal{M}_h} \varrho_h(z)^2. \tag{2.22}$$

(iv) *If both nodes of an element $T \in \mathcal{T}_h$ belong to $\mathcal{M}_h$, T will be marked.*

(v) *For all other nodes in $\mathcal{M}_h$, the multiplicity will be increased if it is smaller than $p + 1$, otherwise the elements which contain one of these nodes $z \in \mathcal{M}_h$, will be marked.*

(vi) *Refine all marked elements $T \in \mathcal{T}_h$ by bisection (insertion of a node with multiplicity one) of the corresponding $\check{T} \in \check{\mathcal{T}}_h$. Use further bisections to guarantee that the new partition $\mathcal{T}_H$ satisfies*

$$\kappa(\check{\mathcal{T}}_H) \leq 2\kappa(\check{\mathcal{T}}_0). \tag{2.23}$$

Update $h \mapsto H$, i.e., replace $\mathcal{T}_h$ by $\mathcal{T}_H$.

Output: Adaptively generated partition $\mathcal{T}_h$ with corresponding solution ϕ_h and error estimator ϱ_h. $\square$

Remark 2.3. (i) *While $\theta = 1$ leads essentially to uniform refinement, $\theta \ll 1$ leads to highly adapted partitions. Note that the smaller θ, the more iterations of the adaptive loop are required. In our experiments below, $\theta = 0.75$ appeared to be an appropriate compromise which led to optimal convergence behavior.*
(ii) *The estimate (2.23) in step (iv) of the adaptive algorithm can be achieved by some extended 1D bisection algorithm from [AFF+13]. The latter guarantees that the overall number of elements is bounded by the sum of elements in the initial partition plus the number of marked elements.* $\square$

3. Numerical experiments

In this section, we empirically investigate the performance of Algorithm 2.2 for Galerkin as well as collocation IGABEM in three typical situations: In Section 3.2, the boundary $\Gamma = \partial\Omega$ is closed and the solution exhibits a generic (i.e., geometry induced) singularity. In Section 3.3, the solution is smooth on $\Gamma = \partial\Omega$, but has certain jumps which require discontinuous ansatz functions. In Section 3.4, we consider a slit problem. In all examples, the exact solution is known. This allows to analyze the reliability and efficiency of the proposed estimators.

The boundary part Γ is parametrised by a NURBS curve γ, i.e., the parametrisation has the special form

$$\gamma(t) = \sum_{i \in \mathbb{Z}} C_i R_{i,p}^{\check{\mathcal{K}}_\gamma, \mathcal{W}_\gamma}(t) \tag{3.1}$$

for all $t \in [a, b]$. Here, $p \in \mathbb{N}$ is the polynomial degree, $\check{\mathcal{K}}_\gamma$ and $\mathcal{W}_\gamma$ are knots and weights as in Section 2.9 and $(C_i)_{i \in \mathbb{Z}}$ are *control points* in $\mathbb{R}^2$ which are periodic for closed $\Gamma = \partial\Omega$.

We choose the same polynomial degree p for our ansatz spaces $\mathcal{X}_h = \widehat{\mathscr{N}^p}(\check{\mathcal{K}}_h, \mathcal{W}_h)$. For the initial knots and weights, we choose $\check{\mathcal{K}}_h = \check{\mathcal{K}}_\gamma$ and $\mathcal{W}_h = \mathcal{W}_\gamma$. As the ansatz spaces are nested, it always holds

$$\gamma_1, \gamma_2 \in \mathscr{N}^p(\check{\mathcal{K}}_h, \mathcal{W}_h)|_{[a,b]}, \tag{3.2}$$

where γ_1, γ_2 denote the first resp. second component of γ. Therefore, this approach reflects the main idea of isogeometric analysis, i.e., the same space is used for the geometry and for the approximation. For adaptive Galerkin IGABEM as well as adaptive collocation IGABEM, we compare uniform refinement, where $\mathcal{M}_h = \mathcal{N}_h$ and hence all elements are refined, and adaptive refinement with $\theta = 0.75$. In addition, we also consider discontinuous piecewise polynomials. Note that this is formally only a special case if $w_j = 1$ for all weights w_j of $\mathcal{W}_h$ and $\#z_j = p + 1$ for all nodes $z_j \in \mathcal{N}_h$.

As basis for the considered ansatz spaces, we use (2.16) resp. (2.17). To calculate the Galerkin matrix, the collocation matrix, the Faermann error estimator, and the

weighted-residual error estimator, we transform the weakly-singular integrands into a sum of a smooth part and a log-arithmically singular part. Then, we use adapted Gauss quadrature to compute the resulting integrals with appropriate accuracy; see [Gan14, Section 5] for details. For the weighted-residual error estimator (1.5), we replace $|\omega_h(z)|$ by the length $|\gamma^{-1}(\omega(z))|$, since this eases the calculation. Note that $|\omega_h(z)| \simeq |\gamma^{-1}(\omega_h(z))|$, where the hidden constants depend only on the parametrization γ.

To calculate, the exact error, we proceed as follows: Let $\phi_h^{\mathrm{gal}} \in \mathcal{X}_h$ be the Galerkin approximation with $\boldsymbol{c_h^{\mathrm{gal}}}$ the corresponding coefficient vector. Let $\phi_h^{\mathrm{col}} \in \mathcal{X}_h$ be the collocation approximation with $\boldsymbol{c_h^{\mathrm{col}}}$ the corresponding coefficient vector. Let $\boldsymbol{V_h^{\mathrm{gal}}}$ be the Galerkin matrix of the h-th step. With the Galerkin orthogonality and the energy norm $\|\phi\|^2 = \langle V\phi\,;\,\phi\rangle$, obtained by Aitken's Δ^2-extrapolation, we can compute the energy error as

$$\begin{aligned}\|\phi - \phi_h^{\mathrm{gal}}\|^2 &= \|\phi\|^2 - \|\phi_h^{\mathrm{gal}}\|^2 \\ &= \|\phi\|^2 - \langle \boldsymbol{V_h^{\mathrm{gal}} c_h^{\mathrm{gal}}}\,;\,\boldsymbol{c_h^{\mathrm{gal}}}\rangle,\end{aligned} \quad (3.3)$$

resp.

$$\begin{aligned}\|\phi - \phi_h^{\mathrm{col}}\|^2 &= \|\phi - \phi_h^{\mathrm{gal}}\|^2 - \|\phi_h^{\mathrm{gal}} - \phi_h^{\mathrm{col}}\|^2 \quad (3.4) \\ &= \|\phi - \phi_h^{\mathrm{gal}}\|^2 - \langle \boldsymbol{V_h^{\mathrm{gal}}}(\boldsymbol{c_h^{\mathrm{gal}} - c_h^{\mathrm{col}}})\,;\,(\boldsymbol{c_h^{\mathrm{gal}} - c_h^{\mathrm{col}}})\rangle.\end{aligned}$$

3.1. Laplace-Dirichlet problem

In the first two examples, we consider the Laplace-Dirichlet problem

$$-\Delta u = 0 \text{ in } \Omega \quad \text{and} \quad u = g \text{ on } \Gamma \qquad (3.5)$$

for given Dirichlet data $g \in H^{1/2}(\Gamma)$ and closed boundary $\Gamma = \partial\Omega$. The problem is equivalent to the integral equation (1.1) with $f = (K + \sigma)g$, i.e.

$$V\phi = (K + \sigma)g \quad \text{on } \Gamma, \qquad (3.6)$$

where

$$Kg(x) := -\frac{1}{2\pi} \int_\Gamma g(y)\partial_{\nu(y)} \log(|x - y|)\,dy \qquad (3.7)$$

denotes the *double-layer integral operator* and $\sigma(x) = 1/2$ for all $x \in \Gamma$ except of the corners, where $\sigma(x) = \alpha/(2\pi)$ with the corresponding interior angle α. The unique solution of (1.1) is the normal derivative $\phi = \partial u/\partial\nu$ of the solution $u \in H^1(\Omega)$ of (3.5). For more details, see e.g. [Ste08, Section 6.3 and 6.6].

3.2. Problem with generic singularity

As first example, we consider the Laplace-Dirichlet problem (3.5) on the pacman geometry

$$\Omega := \left\{ r(\cos(\beta), \sin(\beta)) : 0 \le r < \frac{1}{10}, \beta \in \left(-\frac{\pi}{2\tau}, \frac{\pi}{2\tau} \right) \right\},$$

with $\tau = 4/7$; see Figure 3.1. The geometry is parametrised on $[0, 1]$ by a NURBS curve of degree $p = 2$. We prescribe the exact solution of (3.5) as

$$u(x, y) = r^\tau \cos(\tau\beta)$$

in polar coordinates $(x, y) = r(\cos\beta, \sin\beta)$. We consider the corresponding integral equation (3.6). The normal derivative $\phi = \partial u/\partial\nu$ of u reads

$$\phi(x, y) = \begin{pmatrix} \cos(\beta)\cos(\tau\beta) + \sin(\beta)\sin(\tau\beta) \\ \sin(\beta)\cos(\tau\beta) - \cos(\beta)\sin(\tau\beta) \end{pmatrix} \cdot \nu(x, y) \cdot \tau \cdot r^{\tau - 1}$$

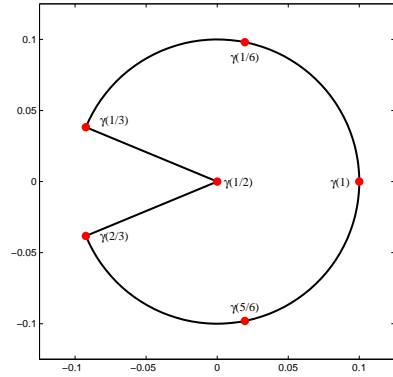and has a generic singularity at the origin.

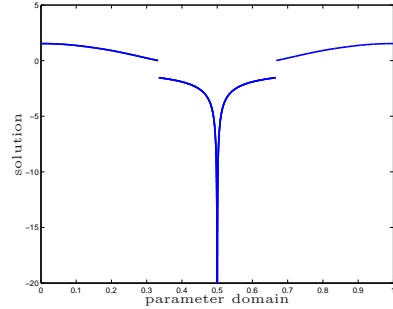Figure 3.1: Geometry and initial nodes for the experiment from Section 3.2.

Figure 3.2: Experiment with singular solution on pacman geometry from Section 3.2. The singular solution $\phi \circ \gamma$ is plotted on the parameter interval, where 0.5 corresponds to the origin, where ϕ is singular.

In Figure 3.2, the solution ϕ is plotted over the parameter domain. The singularity is located at $t = 1/2$ and two jumps are located at $t = 1/3$ rep. $t = 2/3$.

In Figure 3.3, error and error estimators are plotted. All values are plotted in a double logarithmic scale such that the experimental convergence rates are visible as the slope of the corresponding curves. Since the solution lacks regularity, uniform refinement leads to the suboptimal rate $\mathcal{O}(N^{-4/7})$ for the energy error, whereas adaptive refinement leads to the optimal rate $\mathcal{O}(N^{-7/2})$. In each case,
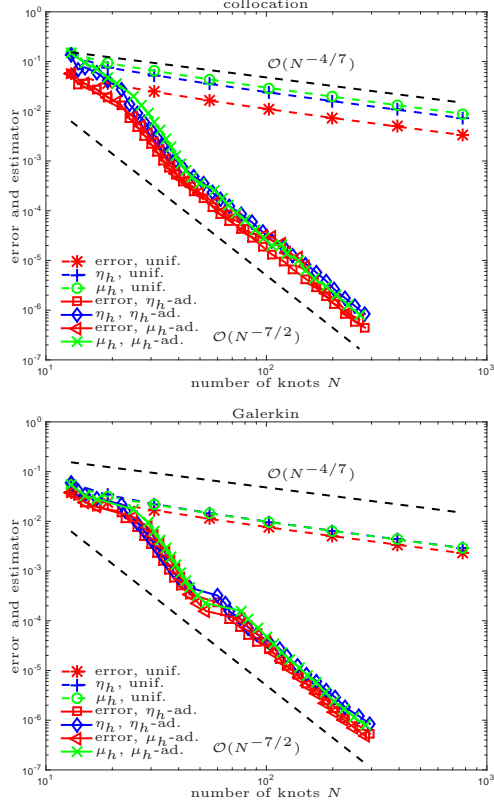
Figure 3.3: Experiment with singular solution on pacman geometry from Section 3.2. Error and estimator are plotted versus the number of knots N. Uniform, η_h-driven and μ_h-driven refinement is considered.

Figure 3.4: Experiment with singular solution on pacman geometry from Section 3.2. The plot shows the efficiency indices $\frac{\rho_h}{\|\!|\phi-\phi_h|\!\|}$ for the estimators $\rho_h \in \{\eta_h, \mu_h\}$, where adaptivity is driven by ρ_h.

Figure 3.5: Experiment with singular solution on pacman geometry from Section 3.2. The errors from all presented adaptive IGABEM strategies are plotted versus the number of knots N.

the curves for the two different estimators η_h and μ_h and the error are parallel. In Figure 3.4, we plot the ratios $\eta_h/\|\!|\phi - \phi_h|\!\|$ resp. $\mu_h/\|\!|\phi - \phi_h|\!\|$. Throughout, these ratios stay between 0.5 and 2.7 which underlines an accurate error estimation for both error estimators. Figure 3.5 shows the errors of all considered adaptive IGABEM strategies. We observe a very similar behaviour.

For adaptive refinement, Figure 3.6 provides a histogram of the knots in $[a, b]$ of the last refinement step for collocation IGABEM with $\rho_h = \mu_h$, for the other adaptive strategies, the output looks similar (not displayed). We see that the algorithm mainly refines the mesh around the singularity at $t = 1/2$. Additionally, the multiplicity at the jump points $t = 1/3$ and $t = 2/3$ appears to be maximal so that the discrete solution ϕ_h also mimics the discontinuities of the exact solution ϕ.

In Figure 3.7, we finally compare standard BEM with discontinuous piecewise polynomials against IGABEM. For the error estimation we use the weighted-residual estimator μ_h. The output looks similar if η_h is used instead (not displayed). All approaches show similar convergence rates, however we clearly observe better multiplicative constants for Galerkin IGABEM and collocation IGABEM than for standard BEM.
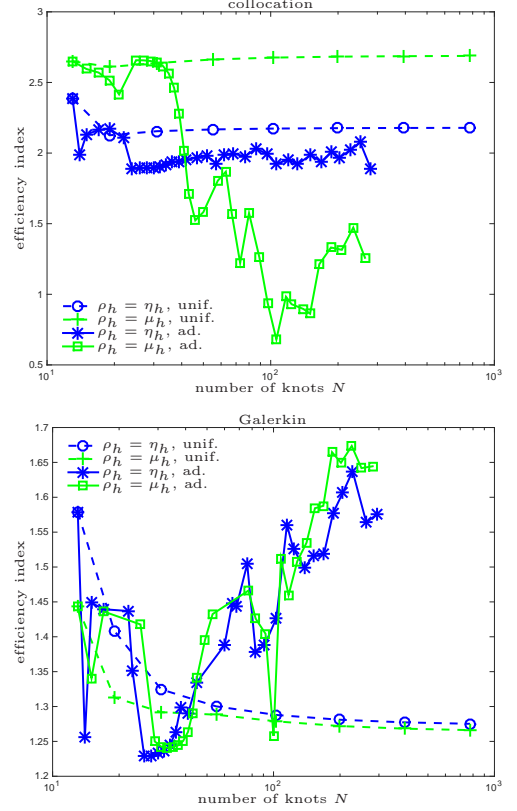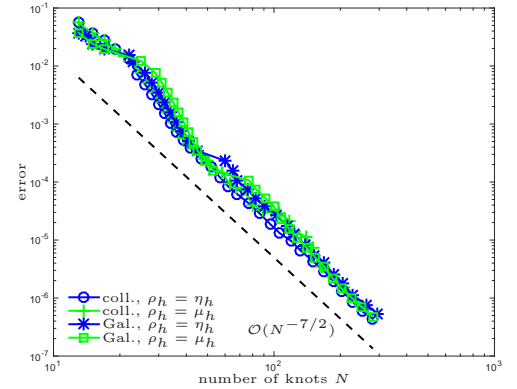
3.3. Adaptive IGABEM for problem with jump solution

As second example, we consider the Laplace-Dirichlet problem (3.5) on the square $\Omega = [0, 1/2]^2$; see Figure 3.8. The geometry is parametrised on $[0, 1]$ by a NURBS curve of degree $p = 1$.

We prescribe the exact solution of (3.5) as

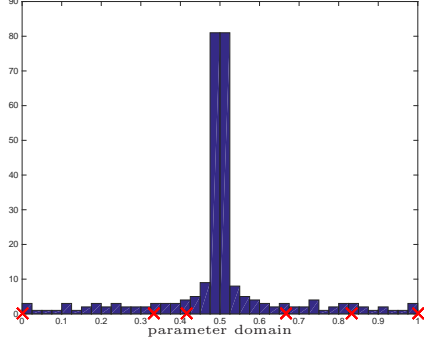$$u(x, y) = \sinh(2\pi x)\cos(2\pi y).$$

Figure 3.6: Experiment with singular solution on pacman geometry from Section 3.2. Histogram of number of knots over the parameter domain. Knots with maximal multiplicity $p + 1 = 3$ are marked.
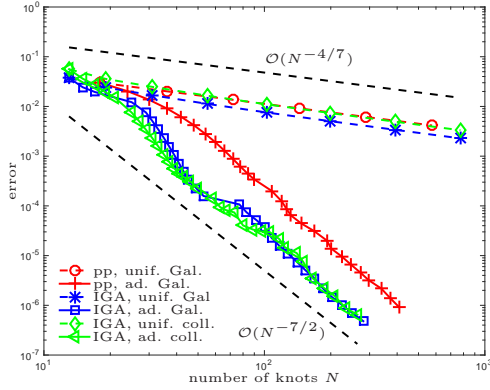

Figure 3.7: Experiment with singular solution on pacman geometry from Section 3.2. The errors from uniform/adaptive BEM with discontinuous piecewise polynomials and uniform/adaptive IGABEM are plotted versus the number of knots N.
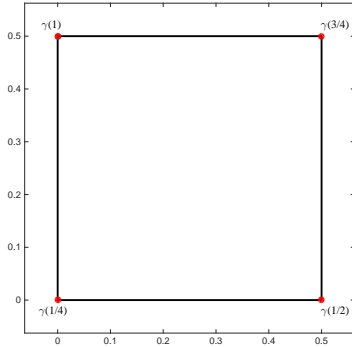

Figure 3.8: Geometry and initial nodes for the experiments from Section 3.3.

We consider the corresponding integral equation (3.6). The normal derivative $\phi = \partial u / \partial \nu$ of u reads

$$\phi(x, y) = 2\pi \begin{pmatrix} \cosh(2\pi x) \cos(2\pi y) \\ \sinh(2\pi x) \cos(2\pi y) \end{pmatrix} \cdot \nu(x, y).$$

It is smooth up to four jumps as can be seen in Figure 3.9.

In Figure 3.10 we plot error and error estimators. The solution $\phi \circ \gamma$ has jumps at the points $t = 1/4$, $t = 1/2$, $t = 3/4$ and $t = 1$ resp. $t = 0$. As the knots $\check{\mathcal{K}}_\gamma$ used for the parametrisation of Γ all have multiplicity one, the functions of the isogeometric start approximation space are continuous at the points $t = 1/4$, $t = 1/2$ and $t = 3/4$. Uniform refinement, where only h-refinement takes place, leads to the suboptimal rate $\mathcal{O}(N^{-1})$ for the energy error, whereas adaptive refinement increases the knot multiplicity at these problematic points and leads again to the optimal rate $\mathcal{O}(N^{-5/2})$. In Figure 3.11, we plot the efficiency indices $\eta_h / \|\phi - \phi_h\|$ resp. $\mu_h / \|\phi - \phi_h\|$. Throughout, these ratios stay between 0.1 and 2.2. Figure 3.12 shows the errors of all considered adaptive IGABEM strategies. We observe that η_h leads to slightly better results than μ_h, while there appears to be almost no difference between Galerkin IGABEM and collocation IGABEM.

In Figure 3.13, standard BEM with discontinuous piecewise polynomials is compared against IGABEM. For adaptivity, we use the weighted-residual estimator μ_h. The output looks similar if the estimator η_h is used (not displayed). We observe that in this example uniform standard BEM is superior to uniform IGABEM. This is of course due to the fact that standard BEM uses ansatz spaces which are discontinuous at the jumps of ϕ. However, with the use of adaptive multiplicity increase this is fixed as can be seen in the convergence plot, where we again see that adaptive IGABEM leads to better results than adaptive standard BEM. It is also interesting that adaptive standard BEM converges with a better multiplicative constant than uniform standard BEM. This is due to the fact that the solution is zero on $[1/4, 1/2]$ and $[3/4, 1]$, wherefore the adaptive algorithm uses only few elements in this area.
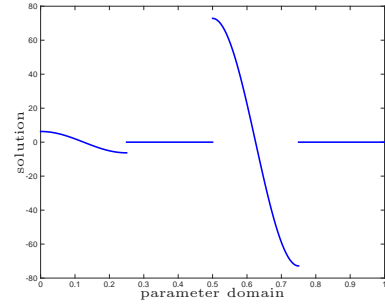

Figure 3.9: Experiment with jump solution on square from Section 3.3. The solution $\phi \circ \gamma$ is plotted on the parameter interval.

3.4. Adaptive IGABEM for slit problem

As last example, we consider a crack problem on the slit $\Gamma = [-1, 1] \times \{0\}$. We parametrize Γ by a NURBS curve of degree $p = 1$. For $f(x, 0) := -x/2$ and the single-layer operator V, the exact solution of (1.1) reads
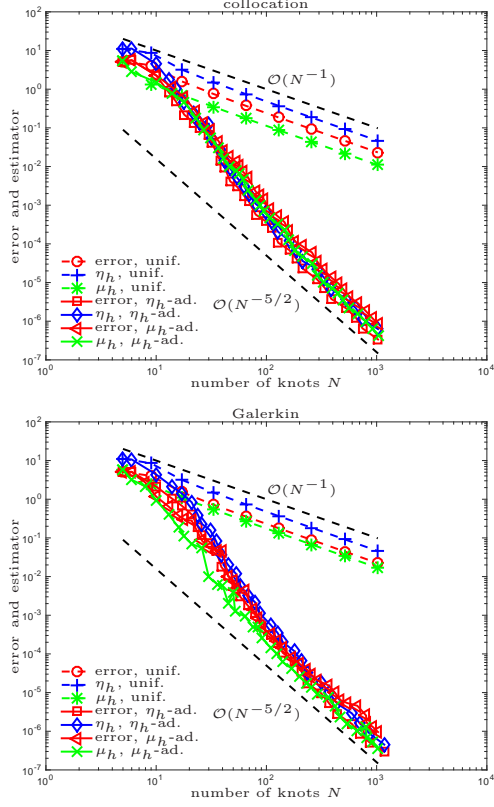
$$\phi(x, 0) = \frac{-x}{\sqrt{1 - x^2}}.$$

Figure 3.10: Experiment with jump solution on square from Section 3.3. Error and estimator are plotted versus the number of knots N. Uniform, η_h-driven and μ_h-driven refinement is considered.

Figure 3.11: Experiment with jump solution on square from Section 3.3. The plot shows the efficiency indices $\frac{\rho_h}{\|\!\|\phi - \phi_h\|\!\|}$ for the estimators $\rho_h \in \{\eta_h, \mu_h\}$, where adaptivity is driven by ρ_h.

Figure 3.12: Experiment with jump solution on square from Section 3.3. The errors from all presented adaptive IGABEM strategies are plotted versus the number of knots N.

Note that $\phi \in \widetilde{H}^{-\varepsilon}(\Gamma) \setminus L^2(\Gamma)$ for all $\varepsilon > 0$ and that ϕ has singularities at the tips $x = \pm 1$.

In Figure 3.15, error and error estimators for the uniform and for the adaptive approach are plotted. The error is obtained via (3.3) resp. (3.4), where $\|\!\|\phi\|\!\|^2 = \pi/4$ is computed analytically. Since the solution lacks regularity, uniform refinement leads to the suboptimal rate $\mathcal{O}(N^{-1/2})$, whereas adaptive refinement leads to the optimal rate $\mathcal{O}(N^{-5/2})$. The curves for the two estimators and the error are again parallel. In Figure 3.17, we plot the efficiency indices $\eta_h/\|\!\|\phi - \phi_h\|\!\|$ resp. $\mu_h/\|\!\|\phi - \phi_h\|\!\|$. Figure 3.16 shows the errors of all considered adaptive IGABEM strategies. Here, η_h-adaptive Galerkin IGABEM and μ_h-adaptive collocation IGABEM lead to the best results. In Figure 3.18 we compare standard BEM against IGABEM, where we use $\rho_h = \mu_h$. While adaptve Galerkin IGABEM and adaptive standard BEM lead to optimal convergence rates, the best results are achieved with adaptive collocation IGABEM.
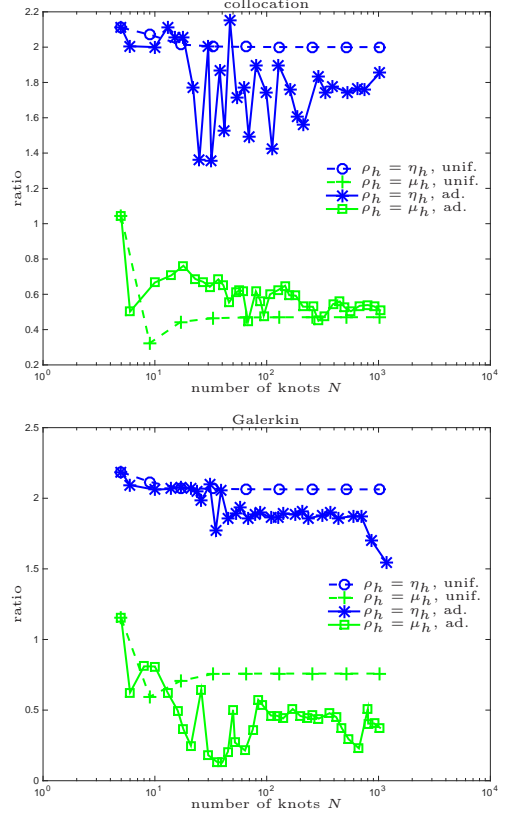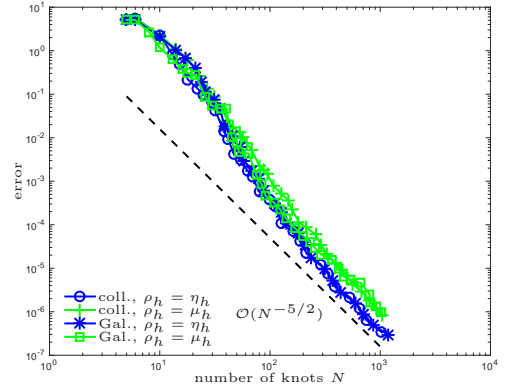
4. A posteriori error estimation for IGABEM

4.1. Main results

For $T \in \mathcal{T}_h$, we inductively define the patch $\omega_h^m(T) \subseteq \Gamma$ of order $m \in \mathbb{N}_0$ by

$$
\begin{aligned}
\omega_h^0(T) &:= T, \\
\omega_h^{m+1}(T) &:= \bigcup \left\{ T' \in \mathcal{T}_h \,:\, T' \cap \omega_h^m(T) \neq \emptyset \right\}
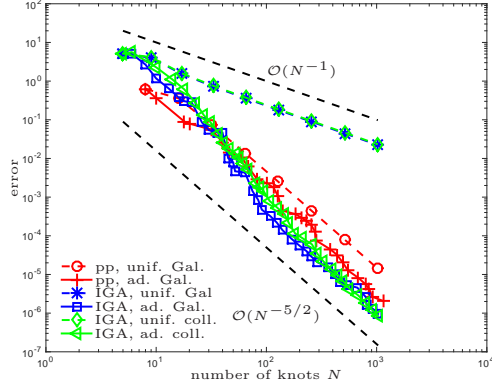\end{aligned}
\tag{4.1}
$$

9

Figure 3.13: Experiment with jump solution on square from Section 3.3. The errors from uniform BEM with discontinuous piecewise polynomials and uniform/adaptive IGABEM are plotted versus the number of knots N.
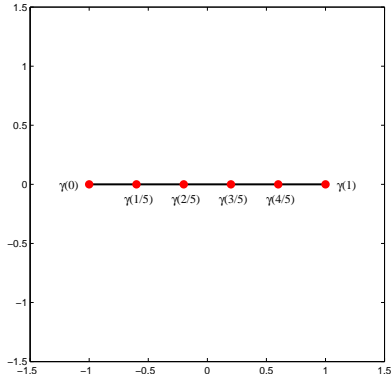

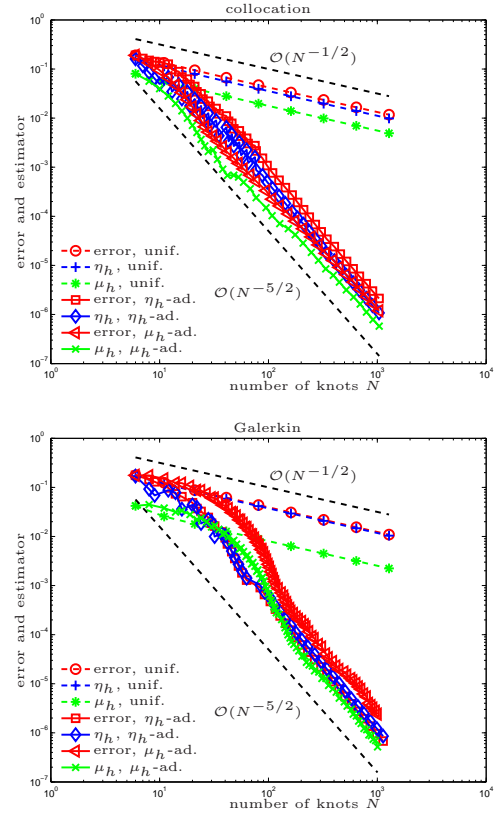Figure 3.14: Geometry and initial nodes for the experiment from Section 3.4.

Figure 3.15: Experiment with singular solution on slit from Section 3.4. Error and estimator are plotted versus the number of knots N. Uniform, η_h-driven and μ_h-driven refinement is considered.
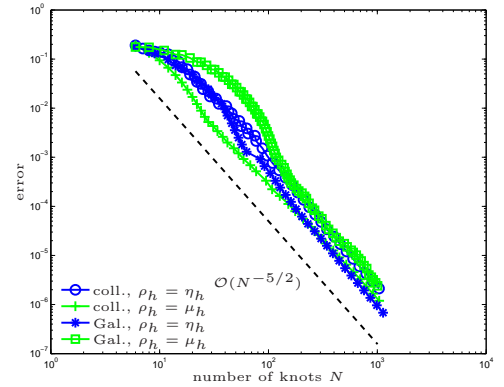

Figure 3.16: Experiment with singular solution on slit from Section 3.4. The errors from all presented adaptive IGABEM strategies are plotted versus the number of knots N.

The main result of Theorem 4.2 requires the following two assumptions on $\mathcal{T}_h$ and $\mathcal{X}_h$ for some fixed integer $m \in \mathbb{N}_0$:

(A1) For each $T \in \mathcal{T}_h$, there exists some fixed function $\psi_T \in \mathcal{X}_h$ with connected support $\mathrm{supp}(\psi_T)$ such that

$$T \subseteq \mathrm{supp}(\psi_T) \subseteq \omega_h^m(T). \qquad (4.2)$$

(A2) There exists some constant $q \in (0, 1]$ such that

$$\|1 - \psi_T\|_{L^2(\mathrm{supp}(\psi_T))}^2 \leq (1 - q) \, |\mathrm{supp}(\psi_T)| \qquad (4.3)$$

for all $T \in \mathcal{T}_h$.

The first theorem shows that these assumptions are, in particular, satisfied for NURBS spaces.

Theorem 4.1 ([FGP15, Theorem 4.4]). *For $p \in \mathbb{N}_0$ and $m := \lceil p/2 \rceil$, the space $\mathcal{X}_h := \widehat{\mathcal{N}^p}(\check{\mathcal{K}}_h, \mathcal{W}_h)$ satisfies the assumptions (A1)–(A2). The constant $0 < q \leq 1$ depends only on $\kappa(\check{\mathcal{T}}_h)$, $\min(\mathcal{W}_h)$, $\max(\mathcal{W}_h)$, p, and γ.* $\qquad \square$

The main result of [FGP15] reads as follows:

Theorem 4.2 ([FGP15, Theorem 3.1]). *For any approximation $\phi_h \in L^2(\Gamma)$, the residual $r_h = f - V\phi_h$ satisfies the efficiency estimate*

$$\eta_h := \Big(\sum_{z \in \mathcal{N}_h} \eta_h(z)^2 \Big)^{1/2} \leq C_{\mathrm{eff}} \, \|\phi - \phi_h\| \qquad (4.4)$$

with $\eta_h(z) := |r_h|_{H^{1/2}(\omega_h(z))}$. If the mesh $\mathcal{T}_h$ and the dis-
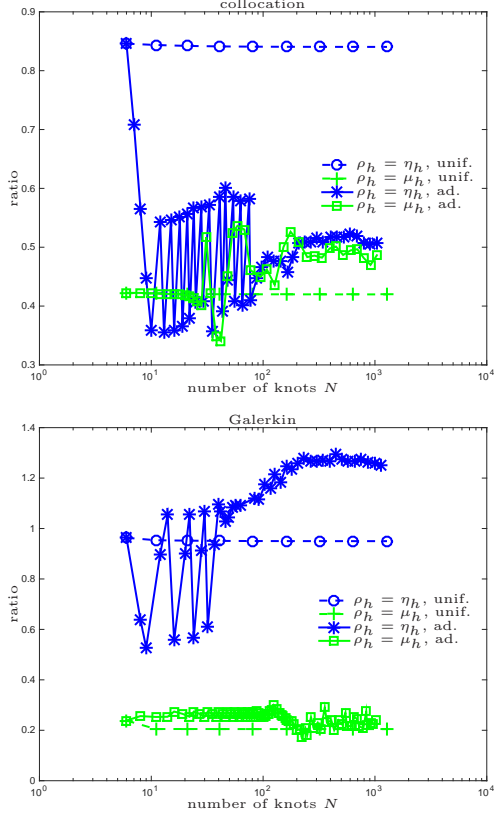
Figure 3.17: Experiment with singular solution on slit from Section 3.4. The plot shows the efficiency indices $\frac{\rho_h}{\|\phi - \phi_h\|}$ for the estimators $\rho_h \in \{\eta_h, \mu_h\}$, where adaptivity is driven by ρ_h.
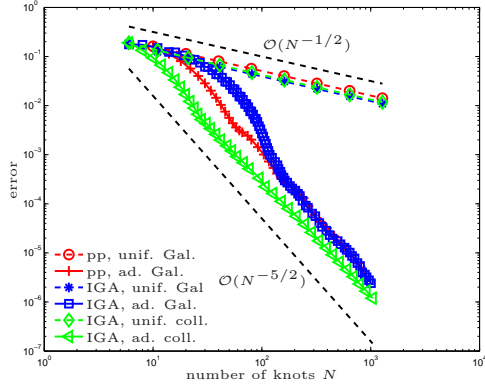

Figure 3.18: Experiment with singular solution on slit from Section 3.4. The errors from uniform BEM with discontinuous piecewise polynomials and uniform/adaptive IGABEM are plotted versus the number of knots N.

crete space $\mathcal{X}_h$ satisfy assumptions (A1)–(A2), the Galerkin solution $\phi_h \in \mathcal{X}_h$ of (1.2) also satisfies the reliability estimate

$$\|\phi - \phi_h\| \leq C_{\mathrm{rel}}\, \eta_h. \qquad (4.5)$$

The constant $C_{\mathrm{eff}} > 0$ depends only on Γ, while $C_{\mathrm{rel}} > 0$ additionally depends on m, $\kappa(\mathcal{T}_h)$, and q. $\qquad \square$

The following two theorems are the mathematical contributions of this work to the field of IGABEM. They apply to both, Galerkin IGABEM as well as collocation IGA-BEM.

Theorem 4.3. *For any approximation $\phi_h \in L^2(\Gamma)$ and $r_h := f - V\phi_h$, the indicator $\eta_h(z) := |r_h|_{H^{1/2}(\omega_h(z))}$ is bounded above by the weighted-residual indicator $\mu_h(z) := |\omega_h(z)|^{1/2}\, \|r_h'\|_{L^2(\omega_h(z))}$*

$$\eta_h(z) \leq \sqrt{2}\, C_\Gamma\, \mu_h(z), \qquad (4.6)$$

where $C_\Gamma > 0$ is the constant from (2.7).

If collocation IGABEM as in Section 2.8 is used, the patch $\omega^{p+1}(T)$ contains a collocation point and therefore a root of the residual r_h, for each $T \in \mathcal{T}_h$. Hence, the condition of the following theorem is fulfilled with $m = p + 1$.

Theorem 4.4. *Suppose that wither $\phi_h \in \mathcal{X}_h$ is the Galerkin solution of (1.2), where $\mathcal{X}_h$ satisfies (A1)–(A2), or that the residual $r_h = f - V\phi_h$ has at least one root in each $\omega_h^m(T)$ for all $T \in \mathcal{T}_h$ and some fixed $m \in \mathbb{N}_0$. Then,*

$$C_{\mathrm{rel}}^{-1}\, \|\phi - \phi_h\| \leq \mu_h := \Big(\sum_{z \in \mathcal{N}_h} \mu_h(z) \Big)^{1/2} \qquad (4.7)$$

with $\mu_h(z) := |\omega_h(z)|^{1/2}\, \|r_h'\|_{L^2(\omega_h(z))}$. The constant $C_{\mathrm{rel}} > 0$ depends only on Γ, m, $\kappa(\mathcal{T}_h)$, and, in the first case, q.

4.2. Proof of Theorem 4.3

We only need the following lemma, whose proof is inspired by [NPV11, Proposition 2.2], where an analogous assertion for norms instead of seminorms is found. The assertion itself is also stated in [CF01, Lemma 7.4] in a more general way. Indeed a similar version of (4.8) holds even for the H^s-seminorm, $0 < s < 1$. However, in [CF01], the proof is only given for the hardest case $1/2 < s < 1$.

Lemma 4.5. *For any connected $\omega \subseteq \Gamma$, whose length satisfies $|\omega| \leq \frac{3}{4}L$ if $\Gamma = \partial\Omega$, there holds*

$$|u|_{H^{1/2}(\omega)}^2 \leq 2\, C_\Gamma^2\, |\omega|\, \|u'\|_{L^2(\omega)}^2 \quad \text{for all } u \in H^1(\Gamma). \quad (4.8)$$

Proof. We recall that for a finite interval $I \subset \mathbb{R}$, $H^1(I)$ coincides with the space of all absolutely continuous functions on $\overline{I}$ with L^2 derivative; see, e.g., [Eva10, page 306]. **Step 1:** First we consider $I = (0,1)$ and prove

$$|u|_{H^{1/2}(I)}^2 \leq 2|u|_{H^1(I)}^2. \qquad (4.9)$$

We use the transformation theorem, with $r = \rho(s - t) + t$ and $s - t = \sigma$, as well as the Cauchy Schwarz inequality

to get

$$|u|^2_{H^{1/2}(I)} = \int_I \int_I \left| \frac{u(s) - u(t)}{s - t} \right|^2 ds\, dt$$

$$= \int_I \int_I \left| \frac{\int_{(0,s)} u'(r)\, dr - \int_{(0,t)} u'(r)\, dr}{s - t} \right|^2 ds\, dt$$

$$= \int_I \int_I \left| \int_I u'(\rho(s - t) + t)\, d\rho \right|^2 ds\, dt$$

$$\leq \int_I \int_I \int_I |u'(\rho(s - t) + t)|^2\, d\rho\, ds\, dt$$

$$= \int_I \int_{(-t, 1-t)} \int_I |u'(\rho\sigma + t)|^2\, d\rho\, d\sigma\, dt.$$

We formally extend u' by zero to $\mathbb{R}$. This and the Fubini theorem lead to

$$|u|^2_{H^{1/2}(I)} \leq \int_I \int_{(-1,1)} \int_I |u'(\rho\sigma + t)|^2\, d\rho\, d\sigma\, dt$$

$$\leq \int_I \int_{(-1,1)} \int_{\mathbb{R}} |u'(\rho\sigma + t)|^2\, dt\, d\sigma\, d\rho$$

$$= \int_I \int_{(-1,1)} \|u'\|^2_{L^2(\mathbb{R})}\, d\sigma\, d\rho = 2|u|^2_{H^1(I)}.$$

Step 2: If $I \subseteq \mathbb{R}$ is an arbitrary finite interval, it holds

$$|u|^2_{H^{1/2}(I)} \leq 2|I||u|^2_{H^1(I)}. \tag{4.10}$$

Without loss of generality, let $I = (c,d)$ be open. We define the function $u_{(0,1)} : (0,1) \to \mathbb{R} : \tau \mapsto u(\tau(d - c) + c)$. Obviously, it holds $u_{(0,1)} \in H^1(0,1)$ with $u'_{(0,1)}(\tau) = (d - c)u'(\tau(d - c) + c)$. The transformation theorem with $s = \sigma(d - c) + c$, $t = \tau(d - c) + c$, and $r = \rho(d - c) + c$, and (4.9) yield

$$|u|^2_{H^{1/2}(I)} = \int_I \int_I \left| \frac{u(s) - u(t)}{s - t} \right|^2 ds\, dt$$

$$= \int_{(0,1)} \int_{(0,1)} \left| \frac{u(\sigma(d - c) + c) - u(\tau(d - c) + c)}{\sigma - \tau} \right|^2 ds\, dt$$

$$= |u_{(0,1)}|^2_{H^{1/2}(0,1)} \leq 2|u_{(0,1)}|^2_{H^1(0,1)}$$

$$= 2 \int_{(0,1)} |u'_{(0,1)}(\rho)|^2\, d\rho = 2(d - c) \int_I |u'(r)|^2\, dr$$

$$= 2|I||u|^2_{H^1(I)}.$$

Step 3: We show (4.8). Let I be a real interval with $\gamma_L(I) = \omega$. Then, (2.8) and (4.10) give

$$|u|_{H^{1/2}(\omega)} = |u|^2_{H^{1/2}(\gamma_L(I))} \leq C_\Gamma^2 |u \circ \gamma_L|^2_{H^{1/2}(I)}$$

$$\leq 2C_\Gamma^2 |\omega| |u \circ \gamma_L|^2_{H^1(I)} = 2C_\Gamma^2 |\omega| \|u'\|^2_{L^2(\omega)}.$$

This concludes the proof. $\qquad\square$

4.3. Proof of Theorem 4.4

We use the following estimate from [Fae00, Lemma 2.3]; see [Gan14, Proposition 2.13] for a detailed proof.

Lemma 4.6. *There exists a constant $C_1 > 0$ such that, for all $u \in H^{1/2}(\Gamma)$, it holds*

$$\|u\|^2_{H^{1/2}(\Gamma)} \leq \sum_{z \in \mathcal{N}_h} |u|^2_{H^{1/2}(\omega_h(z))} + C_1 \sum_{T \in \mathcal{T}_h} h_T^{-1} \|u\|^2_{L^2(T)}. \tag{4.11}$$

The constant only depends on Γ and $\kappa(\mathcal{T}_h)$. $\qquad\square$

Proof of Theorem 4.4. If the residual is orthogonal to some $\mathcal{X}_h$ satisfying (A1)–(A2), the assertion follows at once from Theorem 4.2 in combination with Equation (4.6). If the residual has local roots, we first note that

$$\|\phi - \phi_h\|_{\widetilde{H}^{-1/2}(\Gamma)} \simeq \|f - V\phi_h\|_{H^{1/2}(\Gamma)} = \|r_h\|_{H^{1/2}(\Gamma)}, \tag{4.12}$$

since V is an isomorphism. The hidden constants only depend on Γ.

Taking $u = r_h$ in Lemma 4.6, it only remains to estimate the sum $\sum_{T \in \mathcal{T}_h} h_T^{-1} \|r_h\|^2_{L^2(T)}$. Note that shape regularity yields $|\omega_h^m(T)| \leq (2m+1)\kappa(\mathcal{T}_h)^m h_T$. Replacing T by $\omega^m(T)$, we apply Friedrich's inequality to see

$$\sum_{T \in \mathcal{T}_h} h_T^{-1} \|r_h\|^2_{L^2(T)} \leq \sum_{T \in \mathcal{T}_h} h_T^{-1} \|r_h\|^2_{L^2(\omega_h^m(T))}$$

$$\leq \sum_{T \in \mathcal{T}_h} \frac{|\omega_h^m(T)|^2}{h_T} \|r'_h\|^2_{L^2(\omega^m(T))}$$

$$\leq (2m+1)^2 \kappa(\mathcal{T}_h)^{2m} \sum_{T \in \mathcal{T}_h} h_T \|r'_h\|^2_{L^2(\omega_h^m(T))}$$

$$\leq (2m+1)^3 \kappa(\mathcal{T}_h)^{3m} \sum_{T \in \mathcal{T}_h} h_T \|r'_h\|^2_{L^2(T)}$$

$$\leq (2m+1)^3 \kappa(\mathcal{T}_h)^{3m} \sum_{z \in \mathcal{N}_h} |\omega_h(z)| \|r'_h\|^2_{L^2(\omega(z))}.$$

This concludes the proof. $\qquad\square$

5. Conclusion

5.1. Analytical results

In this work, we considered adaptive BEM for weakly-singular integral equations $V\phi = f$ associated to elliptic PDEs in 2D. As model example served the 2D Laplacian, but the results apply as long as $V : \widetilde{H}^{-1/2}(\Gamma) \to H^{1/2}(\Gamma)$ is an elliptic isomorphism. With the residual $r_h := f - V\phi_h$, we transferred the weighted-residual error estimator

$$\mu_h = \|h^{1/2} r'_h\|_{L^2(\Gamma)} \tag{5.1}$$

proposed in [CS96, Car97] from standard BEM with lowest-order polynomials to IGABEM, where we considered the Galerkin method as well as collocation. For either discretization, we proved that μ_h is reliable

$$\|\phi - \phi_h\| \leq C_{\text{rel}}\, \mu_h; \tag{5.2}$$

see Theorem 4.4. In our preceding work [FGP15], we considered the residual error estimator

$$\eta_h = \Big(\sum_{z \in \mathcal{N}_h} \int_{\omega_h(z)} \int_{\omega_h(z)} \frac{|r_h(x) - r_h(y)|^2}{|x - y|^2} \, dy \, dx \Big)^{1/2} \quad (5.3)$$

proposed in [Fae00]. In [FGP15], we transferred this estimator from standard BEM with piecewise polynomials to IGABEM. Independently of the discretization, we proved the general efficiency estimate

$$\eta_h \leq C_{\mathrm{eff}} \, \|\phi - \phi_h\|, \quad (5.4)$$

while our proof of the converse estimate $\|\phi - \phi_h\| \leq C_{\mathrm{rel}} \, \eta_h$ is restricted to Galerkin IGABEM. However, the combination of (5.2) and (5.4) provides also full error control

$$C_{\mathrm{eff}}^{-1} \, \eta_h \leq \|\phi - \phi_h\| \leq C_{\mathrm{rel}} \, \mu_h \quad (5.5)$$

for collocation IGABEM computations in 2D. Moreover, this estimate implies the global relation $\eta_h \lesssim \mu_h$, and we even proved

$$\mu_h(z) \leq C_{\mathrm{loc}} \, \eta_h(z) \quad \text{for all } z \in \mathcal{N}_h \quad (5.6)$$

for the respective nodal contributions defined in (1.4) resp. (1.5); see Theorem 4.3 which holds independently of the discretization employed.

5.2. Numerical results

We proposed an adaptive algorithm which is capable to steer the mesh-refinement as well as the knot multiplicity in Galerkin and collocation IGABEM computations; see Algorithm 2.2. Numerical experiments in Section 3 underline that generic singularities of the (unknown) exact solutions lead to reduced experimental convergence behavior if the underlying mesh is not appropriately graded. This is a well-known fact for standard BEM with piecewise polynomials, but also applies to IGABEM. Consequently, the gain of adaptive IGABEM (resp. the loss in case of uniform meshes) is huge due to the higher-order ansatz functions of IGABEM, and therefore adaptivity seems to be a must to exploit the full potential of isogeometric analysis. In several numerical experiments, we showed that the proposed algorithm is capable to recover the optimal order of convergence. The gain of IGABEM is that the algorithm chooses smooth NURBS, where the exact solution appears to be smooth, while discontinuities and singularities are well detected and appropriately resolved. Compared to standard BEM with discontinuous piecewise polynomials, this leads to a smaller number of degrees of freedom for comparable accuracies.

For collocation IGABEM as well as Galerkin IGABEM and independently of the (uniform or adaptive) mesh-refinement, we observed that

$$\eta_h \simeq \|\phi - \phi_h\| \simeq \mu_h, \quad (5.7)$$

i.e., both error estimators are efficient and reliable. The efficiency indices $\eta_h / \|\phi - \phi_h\|$ and $\mu_h / \|\phi - \phi_h\|$ appeared to be ≤ 3, i.e., the overestimation of the energy error is very moderate. We note that only the equivalence $\eta_h \simeq \|\phi - \phi_h\|$ for Galerkin IGABEM as well as the bounds $\|\phi - \phi_h\| \lesssim \mu_h$ and $\eta_h \lesssim \|\phi - \phi_h\|$ have thoroughly been proved mathematically.

5.3. Open questions and future work

All considered numerical experiments show optimal convergence of the estimator and the error. Understanding this observation mathematically in the spirit of [CFPP14] is one of our goals for future research. However, it is questionable if an analogous version of the reduction property on refined element domains [CFPP14, (A2)] can be proved for the Faermann estimator η_h. Indeed, this is yet an open problem even for standard BEM with piecewise polynomials; see [FFME+14], where at least convergence of an h-adaptive algorithm with η_h is analyzed. For the weighted-residual error estimator μ_h the axioms of [CFPP14] are satisfied for standard Galerkin BEM with piecewise polynomials, see [CFPP14, Section 5.4]. For collocation IGABEM there remain two challenging mathematical questions: First, one needs further investigation on the unique solvability of the discrete system. Second, the quasi-orthogonality [CFPP14, (A3)] is unclear for collocation methods.

As mentioned, we observed in all numerical experiments reliability as well as efficiency of the used error estimators. However, it remains to mathematically verify the reliability estimate $\|\phi - \phi_h\| \lesssim \eta_h$ for collocation BEM and the efficiency estimate $\mu_h \lesssim \|\phi - \phi_h\| + \mathrm{osc}$, at least for some higher-order oscillation terms osc. Again, these estimates are yet open problems even for standard BEM. For lowest-order Galerkin BEM, the efficiency estimate is proved in [AFF+13, Theorem 4] under additional regularity assumptions on the Dirichlet data g in (3.5).

Finally, the ultimate goal is of course to analyze and apply the estimators η_h and μ_h in 3D Galerkin IGABEM. For 3D one has to consider, e.g., T-splines [SSE+13] or hierarchical B-splines [BG15], because, in contrast to multivariate NURBS, they naturally allow for local mesh refinement. [Fae02] shows that η_h is reliable and efficient for standard BEM with piecewise polynomials, whereas [CMS01] proves reliability for μ_h. In [CFPP14, Section 5.4] optimal convergence of adaptive h-refinement for μ_h is proved. The estimate $\eta_h \lesssim \mu_h$ as well as plain convergence for η_h-based adaptivity is analyzed in [FFME+14]. The transfer of the mentioned results from standard BEM to adaptive IGABEM leaves interesting and challenging questions for future research.

References

[AFF+13] Markus Aurada, Michael Feischl, Thomas Führer, Michael Karkulik, and Dirk Praetorius. Efficiency and optimality of some weighted-residual error estimator for adaptive 2D boundary element methods. *Comput. Methods Appl. Math.*, 13(3):305–332, 2013.

[BG15] Annalisa Buffa and Carlotta Giannelli. Adaptive isogeometric methods with hierarchical splines: error estimator and convergence. *ArXiv preprint arXiv:1502.00565*, 2015.

[Car97] Carsten Carstensen. An a posteriori error estimate for a first-kind integral equation. *Math. Comp.*, 66(217):139–155, 1997.

[CF01] Carsten Carstensen and Birgit Faermann. Mathematical foundation of a posteriori error estimates and adaptive mesh-refining algorithms for boundary integral equations of the first kind. *Eng. Anal. Bound. Elem.*, 25(7):497–509, 2001.

[CFPP14] Carsten Carstensen, Michael Feischl, Marcus Page, and Dirk Praetorius. Axioms of adaptivity. *Comput. Math. Appl.*, 67(6):1195–1253, 2014.

[CHB09] J. Austin Cottrell, Thomas J.R. Hughes, and Yuri Bazilevs. *Isogeometric analysis: toward integration of CAD and FEA*. John Wiley & Sons, 2009.

[CMS01] Carsten Carstensen, Matthias Maischak, and Ernst P. Stephan. A posteriori error estimate and *h*-adaptive algorithm on surfaces for Symm's integral equation. *Numer. Math.*, 90(2):197–213, 2001.

[CS96] Carsten Carstensen and Ernst P. Stephan. Adaptive boundary element methods for some first kind integral equations. *SIAM J. Numer. Anal.*, 33(6):2166–2183, 1996.

[dB86] Carl de Boor. *B (asic)-spline basics*. Mathematics Research Center, University of Wisconsin-Madison, 1986.

[Eva10] Lawrence C. Evans. *Partial differential equations*, volume 19 of *Graduate Studies in Mathematics*. American Mathematical Society, Providence, RI, second edition, 2010.

[Fae00] Birgit Faermann. Localization of the Aronszajn-Slobodeckij norm and application to adaptive boundary element methods. I. The two-dimensional case. *IMA J. Numer. Anal.*, 20(2):203–234, 2000.

[Fae02] Birgit Faermann. Localization of the Aronszajn-Slobodeckij norm and application to adaptive boundary element methods. II. The three-dimensional case. *Numer. Math.*, 92(3):467–499, 2002.

[FFME+14] Michael Feischl, Thomas Führer, Gregor Mitscha-Eibl, Dirk Praetorius, and Ernst P. Stephan. Convergence of adaptive BEM and adaptive FEM-BEM coupling for estimators without *h*-weighting factor. *Comput. Methods Appl. Math.*, 14(4):485–508, 2014.

[FGP15] Michael Feischl, Gregor Gantner, and Dirk Praetorius. Reliable and efficient a posteriori error estimation for adaptive igabem for weakly singular integral equations, 2015.

[Gan14] Gregor Gantner. Isogeometric adaptive BEM. Master's thesis, Vienna University of Technology, 2014.

[HAD14] Luca Heltai, Marino Arroyo, and Antonio DeSimone. Nonsingular isogeometric boundary element method for Stokes flows in 3D. *Comput. Methods Appl. Mech. Engrg.*, 268:514–539, 2014.

[HCB05] Thomas J.R. Hughes, J. Austin Cottrell, and Yuri Bazilevs. Isogeometric analysis: CAD, finite elements, NURBS, exact geometry and mesh refinement. *Comput. Methods Appl. Mech. Engrg.*, 194(39-41):4135–4195, 2005.

[HW08] George C. Hsiao and Wolfgang L. Wendland. *Boundary integral equations*. Berlin: Springer, 2008.

[McL00] William McLean. *Strongly elliptic systems and boundary integral equations*. Cambridge University Press, Cambridge, 2000.

[NPV11] Eleonora Di Nezza, Giampiero Palatucci, and Enrico Valdinoci. Hitchhiker's guide to the fractional sobolev spaces. 04 2011.

[PGK+09] Costas Politis, Alexandros I Ginnis, Panagiotis D Kaklis, Kostas Belibassakis, and Christian Feurer. An isogeometric BEM for exterior potential-flow problems in the plane. In *2009 SIAM/ACM Joint Conference on Geometric and Physical Modeling*, pages 349–354. ACM, 2009.

[PTC13] Michael J. Peake, Jon Trevelyan, and Graham Coates. Extended isogeometric boundary element method (XIBEM) for two-dimensional Helmholtz problems. *Comput. Methods Appl. Mech. Engrg.*, 259:93–102, 2013.

[SBTR12] Robert N. Simpson, Stéphane P. A. Bordas, Jon Trevelyan, and Timon Rabczuk. A two-dimensional isogeometric boundary element method for elastostatic analysis. *Comput. Methods Appl. Mech. Engrg.*, 209/212:87–100, 2012.

[SS11] Stefan A. Sauter and Christoph Schwab. *Boundary element methods*, volume 39 of *Springer Series in Computational Mathematics*. Springer-Verlag, Berlin, 2011. Translated and expanded from the 2004 German original.

[SSE+13] Michael A. Scott, Robert N. Simpson, John A. Evans, Scott Lipton, Stephane P.A. Bordas, Thomas J.R. Hughes, and Thomas W. Sederberg. Isogeometric boundary element analysis using unstructured T-splines. *Comput. Methods Appl. Mech. Engrg.*, 254:197–221, 2013.

[Ste08] Olaf Steinbach. *Numerical approximation methods for elliptic boundary value problems*. Springer, New York, 2008. Translated from the 2003 German original.

[TM12] Toru Takahashi and Toshiro Matsumoto. An application of fast multipole method to isogeometric boundary element method for Laplace equation in two dimensions. *Eng. Anal. Bound. Elem.*, 36(12):1766–1775, 2012.